

Novel Oxindole Based Sensitizers: Synthesis and Application in Dye-Sensitized Solar Cells

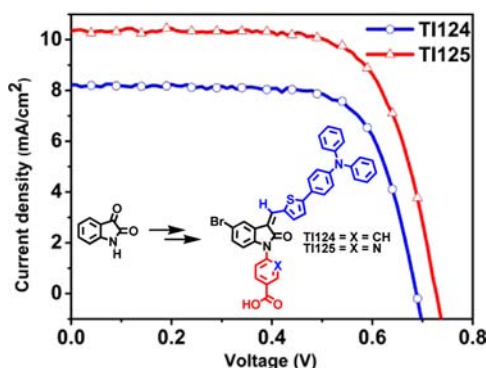
Yogesh S. Tingare,[†] Ming-Tai Shen,[†] Chaochin Su,^{*,‡} Shih-Yu Ho,[‡] Sheng-Han Tsai,[‡]
Bo-Ren Chen,[†] and Wen-Ren Li^{*,†}

Department of Chemistry, National Central University, Chung-Li, Taiwan 32001 and
Institute of Organic and Polymeric Materials, National Taipei University of Technology,
Taipei, Taiwan 10608

ch01@ncu.edu.tw; f10913@ntut.edu.tw

Received May 30, 2013

ABSTRACT



Two novel oxindole sensitizers have been synthesized for dye-sensitized solar cell applications. These new dyes can provide an additional pathway to inject electrons into the photoanode through the partial chelation of their amide carbonyl groups to the TiO₂ surface. Incorporation of an electron deficient pyridine in the acceptor of the T1125 dye was found to enhance the photovoltage and conversion efficiency of the cell.

Energy generation from renewable energy sources has become an important scientific and technological challenge of the 21st century. Clean and abundant solar power is widely recognized as a future energy resource. Accordingly, varieties of light-harvesting devices were developed and the cost-effective dye-sensitized solar cells (DSSCs) have gained particular attention.¹ In DSSCs, the dye is considered the crucial component and research has been focused on optimizing and developing new sensitizers.^{1c,2} In view of limited ruthenium resources, organic sensitizers have attracted considerable interest for their low material

cost, ease of modification, and high molar extinction coefficients.^{2,3} Generally, organic dyes are configured with donor- π -bridge-acceptor (D- π -A) structures for enabling photoinduced charge separation. Various functional groups such as triphenylamine, coumarin, tetrahydroquinoline, cyanine, merocyanine, indoline, phenothiazine, and phenoxazine have been successfully utilized for constructing efficient D- π -A sensitizers for DSSC.^{2,4} Recently, new organic sensitizers representing the "D-A- π -A" configuration were designed to optimize the energy levels of metal-free sensitizers.^{2a} Several kinds of electron-withdrawing moieties such as benzothiadiazole,⁵ benzotriazole,⁶ quinoxaline,⁷ diketopyrrolopyrrole,⁸ and phthalimide⁹ were successfully

[†] National Central University.

[‡] National Taipei University of Technology.

(1) (a) Grätzel, M. *J. Photochem. Photobiol. A* **2004**, *164*, 3. (b) O'Regan, B.; Grätzel, M. *Nature* **1991**, *353*, 737. (c) Robertson, N. *Angew. Chem., Int. Ed.* **2006**, *45*, 2338.

(2) (a) Wu, Y.; Zhu, W. *Chem. Soc. Rev.* **2013**, *42*, 2039. (b) Yin, J.-F.; Velayudham, M.; Bhattacharya, D.; Lin, H.-C.; Lu, K.-L. *Coord. Chem. Rev.* **2012**, *256*, 3008. (c) Hagfeldt, A.; Boschloo, G.; Sun, L.; Kloo, L.; Pettersson, H. *Chem. Rev.* **2010**, *110*, 6595. (d) Mishra, A.; Fischer, M. K. R.; Bäuerle, P. *Angew. Chem., Int. Ed.* **2009**, *48*, 2474.

(3) Yen, Y.-S.; Chou, H.-H.; Chen, Y.-C.; Hsu, C.-Y.; Lin, J.-T. *J. Mater. Chem.* **2012**, *22*, 8734.

(4) (a) Li, C.; Wonneberger, H. *Adv. Mater.* **2012**, *24*, 613. (b) Ning, Z.; Fu, Y.; Tian, H. *Energy Environ. Sci.* **2010**, *3*, 1170. (c) Ning, Z.; Tian, H. *Chem. Commun.* **2009**, 5483.

(5) (a) Zhu, W.; Wu, Y.; Wang, S.; Li, W.; Li, X.; Chen, J.; Wang, Z.-S.; Tian, H. *Adv. Funct. Mater.* **2011**, *21*, 756. (b) Velusamy, M.; Justin Thomas, K. R.; Lin, J. T.; Hsu, Y.-C.; Ho, K.-C. *Org. Lett.* **2005**, *7*, 1899.

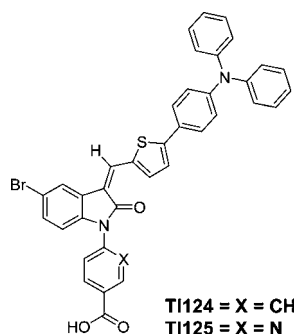
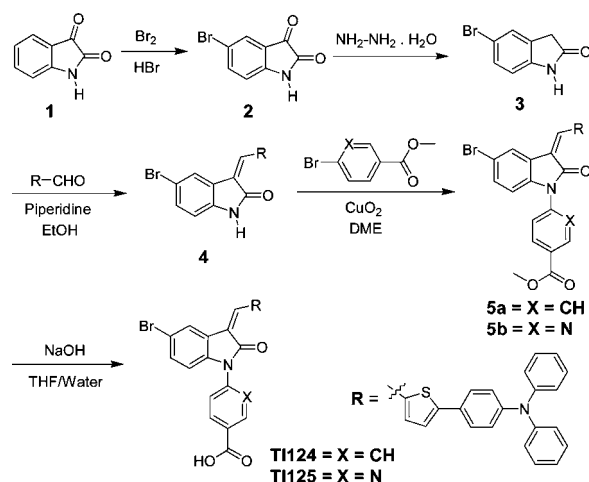


Figure 1. Chemical structures of oxindole based dyes.

incorporated as the additional acceptors in the D–A– π –A sensitizers. Such inclusion of electron-deficient groups was found to improve the photostability of dyes and adjust their energy levels.^{5a} However, the concern hindering the present D–A– π –A dyes is their relatively low photovoltages.^{2a} Owing to the easy molecular tailoring of organic dyes, enhancement in photovoltage could be achieved by assisting fast electron injection through fine-tuning or changing the inserted additional acceptors in the D–A– π –A dyes.

Herein, we report novel organic sensitizers **TI124** and **TI125** (Figure 1) representing the first case of incorporation of oxindoles as the electron-deficient chromophores in sensitizers. The oxindoles are natural indole alkaloids and have abundant use within the pharmaceutical industry.¹⁰ However, their applications as sensitizers have not been explored by other groups. Considering its bicyclic structure consisting of a six-membered benzene ring fused to a five-membered amide containing ring, the oxindole could be a promising candidate in constructing either a D–A–A dye or a D–A– π –A sensitizer. In general, the oxindole based dyes bear beneficial structural characteristics: (1) a possible chelation of the oxindole to the titanium ions on the TiO₂ surface which can help to increase the electron injection yield into the photoanode and might suppress the charge recombination reaction;¹¹ (2) the electron-withdrawing

Scheme 1. Synthesis of **TI124** and **TI125**



amide group is located near the anchoring moiety which can be benefited to accelerate the electron transfer to the TiO₂,¹¹ and (3) the inclusion of a nitrogen atom in the heterocyclic aryl acceptor of the **TI125** sensitizer can provide a better driving force for electron injection (than the **TI124** dye) and thus achieve higher efficiency.¹²

Scheme 1 depicts the synthesis of two newly designed sensitizers **TI124** and **TI125**. Our synthesis started with the selective bromination of isatin (**1**),¹³ followed by a Wolff–Kishner reduction to give 5-bromo-2-oxindole (**3**).¹⁴ A Knoevenagel reaction¹⁵ was then used to condense compound **3** with 5-[4-(diphenylamino) phenyl]thiophene-2-carbaldehyde¹⁶ to yield compound **4** as a single *Z*-isomer.¹⁷ One of the reasons for the predominate formation of the *Z*-isomer is the electrostatic interaction between the carbonyl oxygen of the amide and the partial positively charged sulfur of the thiophene.¹⁵ Ester **5a** and **5b** were synthesized by Ullmann-type amination coupling reactions of compound **4** with 4-bromobenzoic acid methyl ester and 6-bromo-pyridine-3-carboxylic acid methyl ester, respectively. Finally, basic hydrolysis of ester **5a** and **5b** offered sensitizers **TI124** and **TI125**, respectively. Detailed synthetic procedures and characteristic data for all the compounds are provided in the Supporting Information (SI).

The absorption spectra of **TI124** and **TI125** were investigated using UV–vis absorption spectroscopy (Figure 2).

(6) (a) Mao, J.; Guo, F.; Ying, W.; Wu, W.; Li, J.; Hua, J. *Chem.—Asian J.* **2012**, *7*, 982. (b) Cui, Y.; Wu, Y.; Lu, X.; Zhang, X.; Zhou, G.; Miapheh, F. B.; Zhu, W.; Wang, Z.-S. *Chem. Mater.* **2011**, *23*, 4394.

(7) (a) Shi, J.; Chen, J.; Chai, Z.; Wang, H.; Tang, R.; Fan, K.; Wu, M.; Han, H.; Qin, J.; Peng, T.; Li, Q.; Li, Z. *J. Mater. Chem.* **2012**, *22*, 18830. (b) Pei, K.; Wu, Y.; Wu, W.; Zhang, Q.; Chen, B.; Tian, H.; Zhu, W. *Chem.—Eur. J.* **2012**, *18*, 8190. (c) Lu, X.; Feng, Q.; Lan, T.; Zhou, G.; Wang, Z.-S. *Chem. Mater.* **2012**, *24*, 3179. (d) Chang, D.-W.; Lee, H.-J.; Kim, J.-H.; Park, S.-Y.; Park, S.-M.; Dai, L.; Baek, J.-B. *Org. Lett.* **2011**, *13*, 3880.

(8) (a) Qu, S.; Wang, B.; Guo, F.; Li, J.; Wu, W.; Kong, C.; Long, Y.; Hua, J. *Dyes Pigm.* **2012**, *92*, 1384. (b) Qu, S.; Wu, W.; Hua, J.; Kong, C.; Long, Y.; Tian, H. *J. Phys. Chem. C* **2009**, *114*, 1343.

(9) (a) Li, W.; Wu, Y.; Zhang, Q.; Tian, H.; Zhu, W. *ACS Appl. Mater. Interfaces* **2012**, *4*, 1822. (b) Feng, Q.; Lu, X.; Zhou, G.; Wang, Z.-S. *Phys. Chem. Chem. Phys.* **2012**, *14*, 7993.

(10) (a) Silva, J. F. M.; Garden, S. J.; Pinto, A. C. *J. Braz. Chem. Soc.* **2001**, *12*, 273. (b) Sun, L.; Tran, N.; Tang, F.; App, H.; Hirth, P.; McMahon, G.; Tang, C. *J. Med. Chem.* **1998**, *41*, 2588.

(11) Mao, J.; He, N.; Ning, Z.; Zhang, Q.; Guo, F.; Chen, L.; Wu, W.; Hua, J.; Tian, H. *Angew. Chem.* **2012**, *124*, 10011.

(12) Delcamp, J. H.; Yella, A.; Nazeeruddin, M. K.; Grätzel, M. *Chem. Commun.* **2012**, *48*, 2295.

(13) Chaubey, A. K.; Pandeya, S. N. *Int. J. Res. Ayurveda Pharm.* **2011**, *2*, 1763.

(14) Mologni, L.; Rostagno, R.; Brussolo, S.; Knowles, P. P.; Kjaer, S.; Murray-Rust, J.; Rosso, E.; Zamboni, A.; Scapozza, L.; McDonald, N. Q.; Lucchini, V.; Gambacorti-Passerini, C. *Bioorg. Med. Chem.* **2010**, *18*, 1482.

(15) (a) Sun, L.; Tran, N.; Tang, F.; App, H.; Hirth, P.; McMahon, G.; Tang, C. *J. Med. Chem.* **1998**, *41*, 2588. (b) Rumer, J. W.; Dai, S.-Y.; Levick, M.; Biniek, L.; Procter, D. J.; McCulloch, I. *J. Polym. Sci., Part A: Polym. Chem.* **2013**, *51*, 1285.

(16) Liu, W.-H.; Wu, I. C.; Lai, C.-H.; Lai, C.-H.; Chou, P.-T.; Li, Y.-T.; Chen, C.-L.; Hsu, Y.-Y.; Chi, Y. *Chem. Commun.* **2008**, 5152.

(17) Ankati, H.; Akubathini, S. K.; Kamila, S.; Mukherjee, C.; D'Mello, S. R.; Biehl, E. R. *Open Org. Chem. J.* **2009**, *3*, 1.

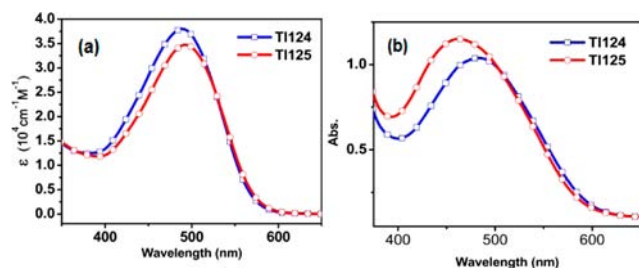


Figure 2. Absorption spectra of **TI124** and **TI125** dyes in CH_2Cl_2 (a) and on films (b).

The absorption spectra of **TI124** and **TI125** dyes (Figure 2a) in CH_2Cl_2 showed strong absorption bands at 488 and 491 nm, respectively. The absorption maximum (λ_{max}) of **TI125** was slightly more red-shifted (ca. 3 nm) than that of **TI124**. Surprisingly, the molar extinction coefficient (ϵ) for **TI124** ($\epsilon = 3.82 \times 10^4 \text{ M}^{-1} \text{ cm}^{-1}$) was a little higher when compared to **TI125** ($\epsilon = 3.45 \times 10^4 \text{ M}^{-1} \text{ cm}^{-1}$). The UV–vis absorption spectra of **TI124** and **TI125** dyes anchored onto the TiO_2 films (Figure 2b) were broadened and blue-shifted when compared to sensitizers in CH_2Cl_2 . To the best of our knowledge, organic dyes featured blue shifts in the absorption peaks when attached onto the TiO_2 surface, and such a phenomenon was attributed to the formation of aggregation of sensitizers or deprotonation of carboxylic acids.^{11,18} In contrast to the solution, the sensitizer **TI125** on film showed higher absorption than the dye **TI124**.

The highest occupied molecular orbital (HOMO) and the lowest unoccupied molecular orbital (LUMO) energy levels play a crucial role in affecting the dye-regeneration and electron-transfer processes in DSSCs. An efficient sensitizer should possess a sufficiently low HOMO energy level for efficient regeneration of the oxidized dye by the electrolyte, whereas the LUMO energy level should be sufficiently high for electron injection into the TiO_2 electrode. We estimated the HOMO and LUMO energy levels of **TI124** and **TI125** from their UV–vis absorption spectra and their cyclic voltammograms to ensure that they were suitable for injecting electrons and dye regeneration after the electron donation.¹⁹ Table 1 reveals that the HOMO energy levels of **TI124** and **TI125** are sufficiently lower than that of the I^-/I_3^- (−4.8 eV) redox potential, and their LUMOs are adequate for efficient electron injection. The HOMO and LUMO energy levels of **TI125** were shifted by 0.21 eV relative to that of the **TI124** dye. Compared to the dye **TI124**, the sensitizer **TI125** with stabilized energy levels can more effectively inject excited electrons into the TiO_2 band and can also be reduced rapidly by the electrolyte.

(18) Tian, H.; Yang, X.; Chen, R.; Pan, Y.; Li, L.; Hagfeldt, A.; Sun, L. *Chem. Commun.* **2007**, 3741.

(19) (a) Cardona, C. M.; Li, W.; Kaifer, A. E.; Stockdale, D.; Bazan, G. C. *Adv. Mater.* **2011**, 23, 2367. (b) Chang, W.-C.; Chen, H.-S.; Li, T.-Y.; Hsu, N.-M.; Tingare, Y. S.; Li, C.-Y.; Liu, Y.-C.; Su, C.; Li, W.-R. *Angew. Chem., Int. Ed.* **2010**, 49, 8161.

Table 1. Electrochemical Properties of **TI124** and **TI125** Dyes

dyes	$\lambda_{\text{max}}/\text{nm}^a$	E_{OX}^b (V vs Fc/Fc^+)	E_{HOMO}^c (eV)	E_{LUMO}^d (eV)	E_{0-0}^d (eV)
TI124	488	0.30	5.10	3.02	2.08
TI125	491	0.51	5.31	3.23	2.08

^a Measured in CH_2Cl_2 . ^b The Ag/AgNO_3 reference electrode was calibrated with a ferrocene/ferrocinium (Fc/Fc^+) redox couple. ^c $E_{\text{HOMO}} = E_{\text{OX}} - E_{\text{Fc}/\text{Fc}^+} + 4.8 \text{ eV}$. ^d $E_{\text{LUMO}} = E_{\text{HOMO}} - E_{0-0}$. The band gap, E_{0-0} , was estimated from the onset of the absorption spectrum measured in CH_2Cl_2 .

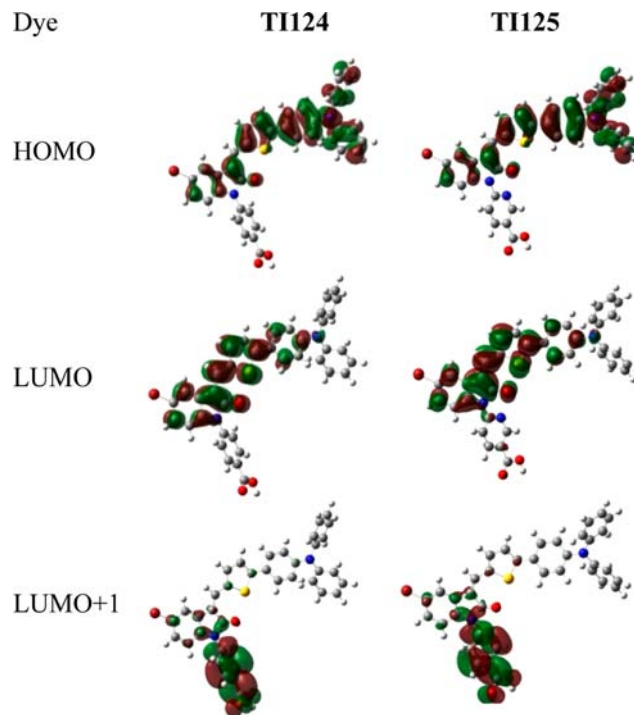


Figure 3. Schematic diagrams of the frontier molecular orbitals of **TI124** and **TI125** calculated at the B3LYP/6-31g (d,p) level of theory.

These results revealed that the additional nitrogen atom incorporated in the aryl acceptor of the dye **TI125** might assist the dye in achieving higher efficiency. To gain more insight into the structural and electronic features of oxindole based dyes, molecular orbital calculations were performed. The HOMO orbitals of **TI124** and **TI125** dyes were localized on the electron-rich donor groups (Figure 3). It is noteworthy that the LUMO levels of **TI124** and **TI125** dyes are confined to the amide portion of the oxindoles and do not feature contributions from the carboxylic groups, while the electron densities of LUMO+1 were populated on the anchoring carboxylic acids. These calculations indicate that the oxindole dyes in this study are poised for effective electron injection through the anchoring carboxylate moieties as well as the amide groups of the oxindoles.

The interaction of sensitizers with the TiO_2 surface and the charge injection are crucial factors affecting the DSSCs

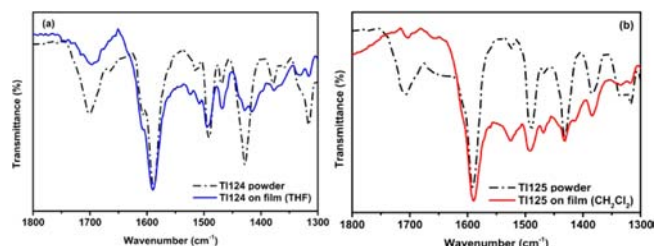


Figure 4. FTIR spectra of the dye powders and dyes adsorbed on films (a) **TI124** (blue) and (b) **TI125** (red).

performance. Prior to making the solar devices, we examined the adsorption pattern of anchored dyes on films to understand the electron transfer mechanism involved in oxindole based sensitizers. FTIR spectra of **TI124** and **TI125** powders and on films were measured and shown in Figure 4. The bands observed at 1702 and 1708 cm^{-1} in the FTIR spectra of **TI124** and **TI125** powders, respectively, can be assigned to amide carbonyl groups of the oxindoles. When the dye was adsorbed on the TiO_2 surface, the peak for $\text{C}=\text{O}$ stretching diminished which indicated the partial chelation of the amide carbonyl group of the oxindole to the titanium ions on the TiO_2 .¹¹ The oxindole based sensitizers might help to improve the photoinduced electron injection yield and gain good photocurrent conversion efficiency.

Figure 5 presents the photocurrent density–voltage curves and the incident photon to current conversion efficiency (IPCE) spectra of DSSCs assembled with multiple layered TiO_2 films with **TI124** and **TI125** sensitizers. Table 2 summarizes the corresponding short-circuit photocurrent densities (J_{sc}), open-circuit voltages (V_{oc}), fill factors (FFs), and solar-to-electricity conversion efficiencies (η). The **TI124**-sensitized DSSC exhibited an overall $\eta = 4.10\%$ with cell parameters of $J_{\text{sc}} = 8.33 \text{ mA cm}^{-2}$, $V_{\text{oc}} = 680 \text{ mV}$, and $\text{FF} = 0.724$. Furthermore, the **TI125** sensitizer with the electron deficient heterocyclic nitrogen containing acceptor improved the V_{oc} by ca. 50 mV. The DSSC based on the **TI125** sensitizer achieved $J_{\text{sc}} = 10.48 \text{ mA cm}^{-2}$, $V_{\text{oc}} = 730 \text{ mV}$, and $\text{FF} = 0.707$, corresponding to an overall $\eta = 5.41\%$. The enhanced η was due to its increase in the V_{oc} which could be attributed to the 0.21 eV lower HOMO energy level of the **TI125** sensitizer, compared to that of the **TI124** dye, which provides a better driving force for dye regeneration. Furthermore, electrochemical impedance spectroscopy (EIS) in the dark (Figure 5c) as well as under illumination (Figure S2 and Table S1 in SI) was performed to analyze the origin of improvement in V_{oc} . The EIS results revealed that the sensitizer **TI125** possessed a higher lifetime and can more effectively suppress the electron recombination than the **TI124** dye. The photocurrent density–voltage curves obtained are in good accord with the corresponding IPCE measurements. The IPCE curve for the DSSC anchored

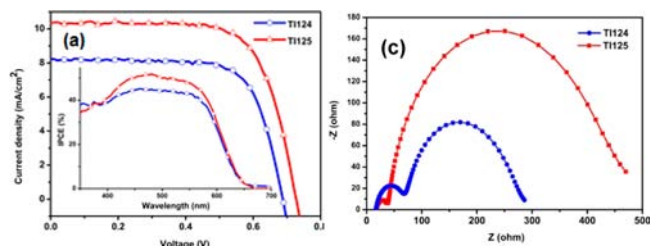


Figure 5. (a) Current versus potential plots. (b) Inset: Monochromatic IPCE spectra. (c) EIS spectra measured in dark of DSSCs based on **TI124** and **TI125** dyes.

Table 2. Photovoltaic Parameters of Devices Incorporating **TI125** and **TI124** Sensitizer

sensitizer	J_{sc} (mA cm^{-2})	V_{oc} (mV)	FF	η (%)
TI124	8.33	680	0.724	4.10
TI125	10.48	730	0.707	5.41

with the **TI124** dye exhibited common broad characteristics that covered the visible spectrum in the range of 400 to 650 nm and reached the maximum IPCE value of 42% at 542 nm (Figure 5b). The **TI125** sensitizer with the pyridine containing acceptor displayed a red-shifted range and increasing IPCE maximum (55% at 542 nm). These results indicate that minor structural modification in the oxindole based sensitizer can effectively alter the physical parameters and the overall photoelectric conversion efficiency of the solar cell.

In conclusion, we have demonstrated the first case of successful usage of oxindoles for constructing sensitizers for DSSC applications. These newly developed dyes ensured an effective electron transfer and suppression of a charge recombination reaction due to the partial chelation of their amide carbonyl groups to the TiO_2 surface. The inclusion of electron deficient pyridine in the acceptor of the **TI125** dye exhibited enhancement in V_{oc} and resulted in higher overall conversion efficiency than the **TI124** sensitizer. Our finding offers an alternative approach for future rational dye design and will help to foster interest in the exploration of oxindole based sensitizers for application in DSSCs.

Acknowledgment. We thank the National Science Council, ROC, for financial support (Grants NSC 100-2113M-008-004-MY3 and NSC 98-2113M-027-003-MY3).

Supporting Information Available. Details of experimental procedures, synthesis and characterization of compounds. This material is available free of charge via the Internet at <http://pubs.acs.org>.

The authors declare no competing financial interest.